

# Prediction performance of space weather forecast centers following the extreme events of October and November 2003

Cary Oler

Solar Terrestrial Dispatch, Stirling, Alberta, Canada

Received 25 February 2004; revised 16 April 2004; accepted 28 April 2004; published 5 August 2004.

[1] A review and analysis of the five strongest interplanetary coronal mass ejection (ICME) events of late October and early November 2003 (the strongest events of the “Halloween” epoch) are studied with respect to the prediction performance of five space weather forecast centers. Accurate time-of-arrival predictions and rapid responses to the upstream detection of strong ICMEs are of paramount importance to critical infrastructures such as power companies. Prediction and performance analysis results indicate that (1) the average time-of-arrival error for all forecast centers was 9.26 hours, which is consistent with the guidance errors associated with the leading shock propagation prediction models; (2) time-of-arrival predictions from Solar Terrestrial Dispatch (STD) surpassed all others in accuracy, with an average time-of-arrival prediction error of 1.22 hours; (3) overall, the strongest ICME impact events of 29 and 30 October were the most poorly predicted; (4) the most accurate shock propagation prediction model operated by the Geophysical Institute of the University of Alaska Fairbanks was the HAFv.2 model; and (5) STD provided the most rapid notification to the Northeast Power Coordinating Council concerning the detection and imminent arrival of most of the ICMEs. A better method of conveying time-of-arrival prediction information is presented that may be more easily digested by consumers of space weather services. *INDEX TERMS:* 2722 Magnetospheric Physics: Forecasting; 2788 Magnetospheric Physics: Storms and substorms; 2409 Ionosphere: Current systems (2708); 2139 Interplanetary Physics: Interplanetary shocks; *KEYWORDS:* prediction, GIC, Halloween, performance, storm, CME

*Citation:* Oler, C. (2004), Prediction performance of space weather forecast centers following the extreme events of October and November 2003, *Space Weather*, 2, S08001, doi:10.1029/2004SW000076.

## 1. Introduction

[2] Significant solar activity can have strong impacts on technology and infrastructure systems [Lambour *et al.*, 2003]. The severe geomagnetic storm and associated province-wide power blackout in Quebec on 13 and 14 March 1989 [Czech *et al.*, 1992] forms the historical basis for illustrating the deleterious effects of strong space weather activity on critical infrastructure systems such as those in the Northeast Power Coordinating Council (NPCC) region (Figure 1), which has been historically sensitive to space weather storms and geomagnetically induced currents (GICs).

[3] It is now widely recognized that most intense geomagnetic storms are caused by high-velocity coronal mass ejections [Tsurutani *et al.*, 1988; Gosling *et al.*, 1991; Richardson *et al.*, 2001; Yurchyshyn *et al.*, 2004] associated with extended periods (several hours) of strong southward (less than  $-10$  nT) interplanetary magnetic fields (IMFs) [Gonzalez and Tsurutani, 1987; Gonzalez *et al.*, 1994]. The strength of the IMF, and to a lesser but still notable degree the strength of the southward component, has been correlated with interplanetary coronal mass ejection (ICME) velocity [Gonzalez *et al.*, 1998; Lindsay *et al.*, 1999; Yurchyshyn *et al.*, 2004]. Thus high-velocity Earthward directed ICMEs have the greatest potential to produce the strongest geomagnetic storms.

[4] Whether a high-velocity ICME succeeds in producing an intense geomagnetic storm depends on the presence of strong southward magnetic fields imbedded within the sheath region [Tsurutani *et al.*, 1988; Gosling and McComas, 1987] and/or the core (e.g., the magnetic cloud) of the ICME [Gonzalez *et al.*, 1998]. The arrival of these fields at the Earth can produce strong magnetospheric current systems minutes to hours after the initial impact of the ICME shock front (depending on where in the ICME the southward fields reside). Thus, although the time of arrival of an ICME is not by itself sufficient to predict magnetic storm effects, it is sufficient to predict when strong ICMEs may first begin impacting vulnerable industries such as power grids. For example, the initial shock-driven impact of ICMEs can produce sudden magnetic impulses [Siscoe *et al.*, 1968; Ogilvie *et al.*, 1968; Araki, 1977; Gosling *et al.*, 1991; Russell *et al.*, 1994] that can drive ground-induced currents through power grids around the world nearly simultaneously. These are reasons why power (and other) industries vulnerable to space weather are heavily concerned with the accurate prediction of the arrival time of significant ICME disturbances. This study therefore concentrates on the shock time-of-arrival predictions of the 24 October to 4 November events as a significant indicator of space weather forecast center prediction performance.



Figure 1. Domain of the NPCC control regions.

[5] To be included in this study, a forecast center must have provided prediction information for each of the five strongest ICME events of this epoch. In addition, each prediction must have been time or date stamped and placed in the public domain prior to the arrival of the ICMEs. Suitable prediction distribution methods include e-mail distribution lists and publicly accessible Web pages.

[6] For this study, the predictions from the following space weather forecast centers were examined for suitability.

[7] 1. Space Environment Center (SEC): The world warning space weather agency distributes prediction information via e-mail distribution lists as well as a publicly accessible Web site ([www.sec.noaa.gov](http://www.sec.noaa.gov)). SEC is also a secondary source of prediction information for the NPCC.

[8] 2. Solar Terrestrial Dispatch (STD): The primary space weather forecast center for the NPCC region distributes prediction information via e-mail distribution lists as well as a publicly accessible Web site ([www.spacew.com](http://www.spacew.com)).

[9] 3. Ionospheric Prediction Service (IPS) Radio and Space Services: A regional warning center in Australia distributes prediction information via e-mail distribution lists as well as a publicly accessible Web site ([www.ips.gov.au](http://www.ips.gov.au)).

[10] 4. Geophysical Institute (GI) of the University of Alaska Fairbanks and Exploration Physics International: The research group associated with these organizations produces unofficial “fearless forecasts” jointly with Space Environment Center (SEC)/National Oceanic and Atmospheric Administration researchers that are based on the results of evolving kinematic and semiempirical models of solar wind flows. This group is not an official “forecast center” but rather a research group working on improving the performance and operational parameters of several prominent shock propagation models. Their predictions are designed to be objective with minimal bias. They distribute their predictions through an e-mail distribution list, and the results of their predictions are also publicly available through their Web site ([gse.gi.alaska.edu](http://gse.gi.alaska.edu)). The

predictions from this group of researchers will hereinafter be referred to as the GI predictions.

[11] 5. Solar Influences Data Center (SIDC): A regional warning center in Belgium for the European region produces predictions that are distributed to recipients through e-mail distribution lists and also publicly through its Web site ([sidc.oma.be](http://sidc.oma.be)).

[12] 6. Geological Survey of Canada (GSC): A regional warning center distributes prediction information via a publicly accessible Web site ([www.spaceweather.gc.ca](http://www.spaceweather.gc.ca)). It is also a secondary source of prediction information for the NPCC. Unfortunately, documented time-of-arrival predictions do not appear to have been produced. As a result, the GSC has been excluded from the bulk of this study.

[13] 7. Metatech Corporation (MC): A commercial space weather provider for a power company in the United Kingdom provides publicly available space weather advisories through its Web site ([www.metatechcorp.com](http://www.metatechcorp.com)). Unfortunately, MC advisory notices during this period did not contain sufficient information or were too ambiguous to determine specific time-of-arrival prediction dates for many of the events studied. The predictions from MC are therefore not suitable for inclusion in this study.

[14] The first five space weather forecast centers enumerated above provided suitable prediction information to be included in this study. This study does not discuss the observed effects of the storm activity of October and November on the power grids in the NPCC region. A separate paper is being prepared for publication that will address those impacts.

[15] A brief examination of the solar drivers responsible for the strong ICME events of this epoch is presented in section 2. The time-of-arrival predictions of each forecast center are then examined along with the best and worst predictions in section 3. In section 4 we examine the maximum lead time performance of STD, SEC, and IPS (where STD and SEC rendered services directly to the NPCC). In section 5 we introduce the use of impact prediction windows and discuss their usefulness to space weather consumers.

## 2. Solar Sources of the Extreme Events of October and November 2003

[16] Solar activity intensified to high levels from mid-October through early November 2003 following the emergence of three very large and active sunspot groups (Figure 2). Between 19 October and 4 November these groups were associated with some of the most intense solar activity on record. X-ray flare emissions broke long-standing records. The geomagnetic storms of 29 and 30 October were the most intense of solar cycle 23 and were ranked 6th and 16th, respectively, on the “Top 30” list assembled by SEC for the events commencing from 1936 (SEC Power Point presentation, “Post event review for October 19th–November 17th events,” 21 November 2003, hereinafter referred to as SEC, 2003). The intensity and frequency of the solar X-ray activity are illustrated in the plot of Figure 3.

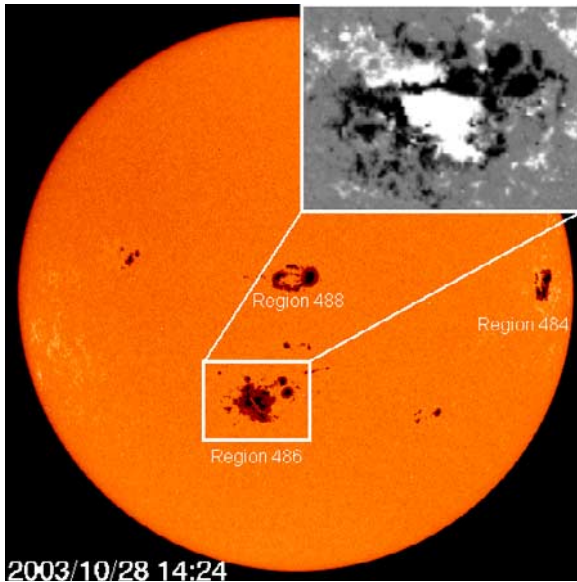


**Figure 2.** Map of active regions just after the large X17/4B proton flare of 28 October and the associated geoeffective ICME from region 486. Images courtesy of Solar and Heliospheric Observatory Michelson Doppler Imager.

[17] Region 10484 (hereinafter referred to as region 484) was the first influential sunspot complex to rotate into view around the northeastern solar limb on 18 October 2003. It grew exceptionally rapidly and produced several energetic solar flares on 19 October, including the first X-class flare in four months (since 15 June 2003), which was successfully (and solely) predicted a little over 12 hours earlier by Solar Terrestrial Dispatch. This spot

complex formed and maintained a strong magnetic delta configuration throughout its passage across the solar disk and unleashed several additional strong solar flares.

[18] Region 10486 (or 486) rotated into view around the southeastern solar limb on 22 October. This region matured as it rotated toward the central solar meridian and quickly asserted itself as the most prolific flare producer of the trio of large spot groups. Multiple magnetic delta configurations were evident in this region (see Figure 2) that supported the eruption of multiple intense X-class solar flares.

[19] Region 10488 (or 488) emerged on the visible disk north and slightly west of region 486 on 27 October. However, it remained comparatively quiet until it approached the western solar limb and did not produce any significant ICMEs.

[20] During the period of 22 October to 4 November, there were nine strong partial and/or full halo coronal mass ejections determined by the Solar and Heliospheric Observatory (SOHO) spacecraft science team. Eight of these events were determined as “front-sided.” Total magnetic field data from the Advanced Composition Explorer (ACE) satellite shows eight relatively well defined transient disturbances in the solar wind during this same time interval (see Figure 4).

[21] Solar wind velocity, density, and temperature data were not available for several of the strongest events because of proton contamination of the ACE Solar Wind, Electron, Proton, and Alpha Monitor (SWEPAM) sensors. Thus only the total interplanetary magnetic field (IMF) strength values were used to sort the ICMEs by strength. The five strongest and best defined ICMEs used in this study (all events with peak IMF magnitudes above 20 nT) are listed in Table 1, sorted according to their dates of occurrence and ranked according to IMF strength. These

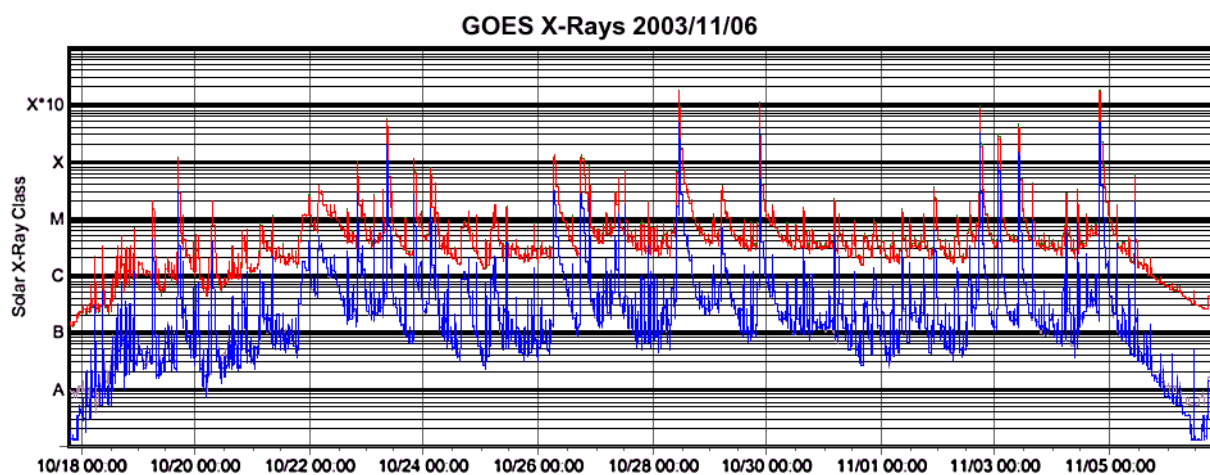


**Figure 3.** X-ray flare activity from 19 October through 4 November. Note the rapid ascent and decay of the background X-ray flux as the active regions appeared, matured, and then rotated out of view behind the west limb. The primary geoeffective solar events occurred between 22 October and 2 November.

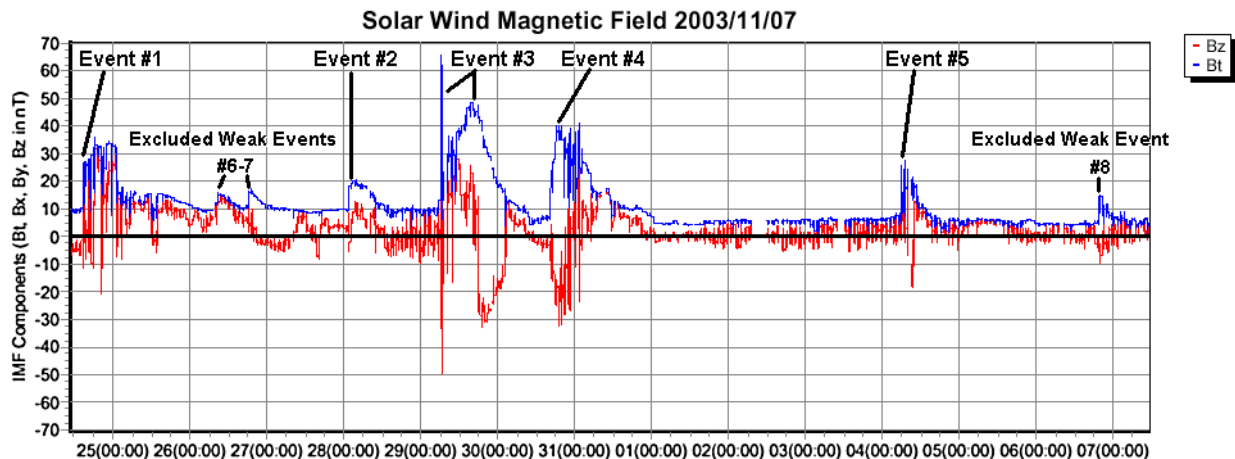


Figure 4. Interplanetary magnetic field data as measured by the ACE spacecraft for the events of 24 October through 6 November. Each event is ranked according to strength by sorting the observed peak total magnetic field magnitudes ( $B_t$ ). Since we are primarily concerned with the prediction performance of the most extreme ICME events, only those events with total magnetic field values that peaked above 20 nT are considered in this study. The events satisfying this criteria are identified as events 1–5 and are listed in Table 1.

five selected events were the only ones associated with periods of severe planetary geomagnetic storm activity (planetary  $K_p$  indices of 7– or greater).

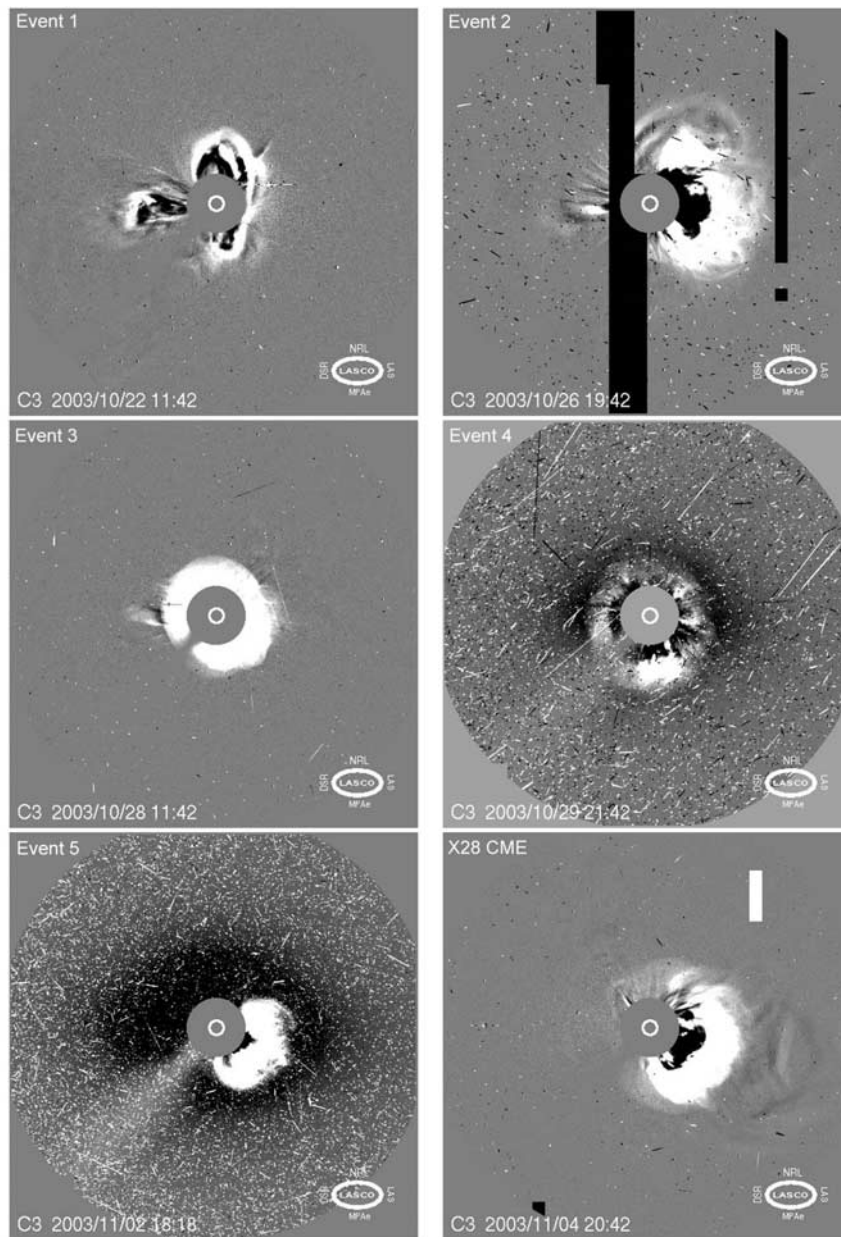
[22] Table 1 and Figures 5 and 6 illustrate the widely varying characteristics, locations, and inferred trajectories of each of the solar driver events. The variances in the characteristics and trajectories of the five selected events should be sufficient to reveal the skill of each forecast center in assessing and predicting their respective impacts.

A map of the physical locations of each of the events in Table 1 is illustrated in Figure 6.

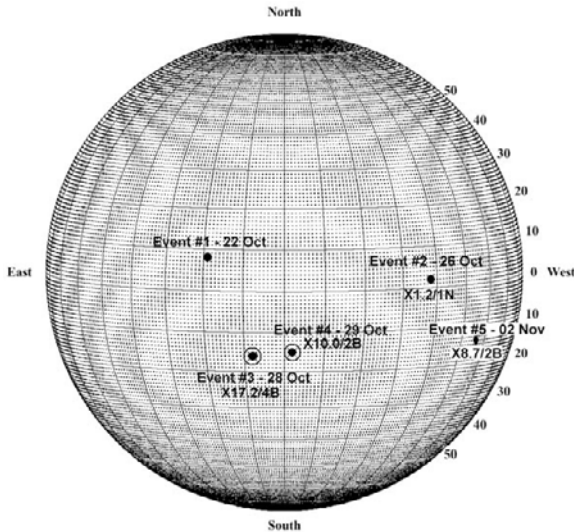
[23] Note that although the most extreme coronal mass ejection having a plane-of-sky velocity of  $2381 \text{ km sec}^{-1}$  was observed on 4 November in association with the X28 solar flare event (as extrapolated from saturated GOES X-ray data by SEC and more recently estimated as an X40-X50 event through its X-ray impact on the Earth's ionosphere [Thomson *et al.*, 2004]), the Earth-bound impact

Table 1. Characteristics of the Five Strongest ICMEs

Event	Rank	ICME Ejection Date and Time (From C2)	Associated Solar Event (Type II Onset)	Integrated X-Ray Flux, $\text{J m}^{-2}$	SSC or Sudden Impulse at Earth Date and Time	Estimated Type II Shock Velocity, $\text{km s}^{-1}$	Estimated Plane-of-Sky Velocity (SOHO), $\text{km s}^{-1}$
1	3	22 Oct. 2003 0745 UTC	22 Oct. 2003 0938 UTC region 484, multiple X ray, N08E19	multiple peaks; complex	24 Oct. 2003 1529 UTC	650	898
2	5	26 Oct. 2003 1754 UTC	26 Oct. 2003 1735 UTC region 484, X1.2/1N, N02W38	$6.3 \times 10^{-1}$	28 Oct. 2003 0206 UTC	950	1432
3	1	28 Oct. 2003 1054 UTC	28 Oct. 2003 1102 UTC region 486, X17.2/4B, S16E08	$1.8 \times 10^0$	29 Oct. 2003 0613 UTC	1250	2125
4	2	29 Oct. 2003 2054 UTC	29 Oct. 2003 2042 UTC region 486, X10.0/2B, S15W02	$8.7 \times 10^{-1}$	30 Oct. 2003 1640 UTC	775	1948
5	4	2 Nov. 2003 1730 UTC	02 Nov. 2003 1714 UTC region 486, X8.7/2B, S14W56	$9.1 \times 10^{-1}$	4 Nov. 2003 0627 UTC	1691	1826



**Figure 5.** Large Angle and Spectrometric Coronagraph (LASCO) experiment C3 images illustrating the relative trajectories of each of the ICMEs associated with the events in Table 1. The event following the X28/SEC or X40-50/Thomson flare of 4 November is also shown for completeness, even though the Earth-bound impact was too weak to appear on our list of the five strongest events. The image of 2 November does not show the full halo coronal mass ejection very well because of strong proton contamination of the LASCO camera. As these images suggest, the trajectories of these coronal mass ejection events varied significantly with primary radial components directed toward the Earth and at apparent near-right angles to the Earth.



**Figure 6.** Probable solar source locations of the five strongest ICME impacts. The two solar events associated with the strongest ICME impacts are indicated with circled dots.

of that event was ranked as the weakest because of the poor location of the solar driver on the west limb and has therefore been excluded from this study.

### 3. Time-of-Arrival Prediction Analysis

[24] The five space weather forecast center predictions are listed in Tables 2–6. Only the first official time-of-arrival predictions issued by each forecast center are used in order to prevent the introduction of undue bias and to ensure as accurate a comparison as possible.

[25] Most forecast centers are careful when it comes to specifying time-of-arrival estimates. Time-of-arrival predictions are very difficult to accurately determine, and there are always a number of hours of uncertainty. As a result, most forecast centers indicate predicted times of

arrivals that span a portion of a UTC day. For example, SEC’s prediction for 26 October (a copy of this report is available from sec@sec.noaa.gov) stated

Geophysical activity forecast: the geomagnetic field is expected to be quiet to active all three days, with possible minor storm conditions on day two due to a partial halo CME from the X1.2 flare observed today at 0654 UTC.

[26] Thus the only useful time-of-arrival prediction information from SEC for this event is a 24-hour window centered on “day two,” corresponding to the UTC day of 28 October. This is a common trait observed with most forecast centers.

[27] The uncertainties in the time-of-arrival statements given by SEC, IPS, and SIDC make it difficult to determine preferred times of arrivals. For these forecasts we look at the wording used in the predictions and take the best reasonable estimate. For example, IPS predicted that the disturbance of 28 October would arrive some time during the “2nd half of the UT day of 28 October.” We therefore assigned this event a “most reasonable” time of arrival of 1800 UTC, which is the midpoint of the second half of the UTC day. The resulting prediction error is subject to some uncertainty (in this case, roughly 6 hours) but should represent a reasonable estimate given the available form of the prediction statement. Later in this study, we look at the results of adjusting the most reasonable times of arrivals in order to minimize the errors within the constraints imposed by the given forecast statements.

[28] The researchers associated with the GI make multiple objective predictions using a suite of solar wind shock propagation models, including the shock time of arrival (STOA) model [Dryer and Smart, 1984; Smart et al., 1984, 1986; Smart and Shea, 1985; Lewis and Dryer, 1987] and the revised STOA-2 model [Moon et al., 2002; Vlasov, 1988, 1992], the interplanetary shock propagation model (ISPM) [Smith and Dryer, 1995], and the HAFv.2 model [Fry, 1985; Fry et al., 2001; Hakamada and Akasofu, 1982].

[29] To make use of the GI predictions in this study, it is necessary to establish a most reasonable time-of-

**Table 2.** Prediction Performance of Solar Terrestrial Dispatch<sup>a</sup>

Actual Observed ICME Impact Date	Most Reasonable Impact Prediction	Issue Time of Prediction	Prediction Error	Minimized Error	$K \geq 6$ or 7 Alert Date Issued	Lead Time Between Alert and ICME Arrival
24 Oct. 2003 1529 UTC	24 Oct. 2003 1400 UTC	22 Oct. 2003 1845 UTC	1 hour 29 min	1 hour 29 min	24 Oct. 2003 1522 UTC	+7 min
28 Oct. 2003 0206 UTC	28 Oct. 2003 0300 UTC	27 Oct. 2003 0630 UTC	29 min 54 min	54 min	none issued or required	not applicable; no alert issued
29 Oct. 2003 0613 UTC	29 Oct. 2003 0800 UTC	28 Oct. 2003 1630 UTC	1 hour 47 min	1 hour 47 min	29 Oct. 2003 0603 UTC	+10 min
30 Oct. 2003 1640 UTC	30 Oct. 2003 1800 UTC	30 Oct. 2003 0405 UTC	1 hour 20 min	1 hour 20 min	alert in progress continued from previous event	separate notice of shock arrival sent out at 1657 UTC
4 Nov. 2003 0627 UTC	4 Nov. 2003 0700 UTC	2 Nov. 2003 2250 UTC	33 min	33 min	4 Nov. 2003 0608 UTC	+19 min

<sup>a</sup>Average time-of-arrival prediction error was 1 hour 13 min.

Table 3. Prediction Performance of Space Environment Center<sup>a</sup>

Observed ICME Impact Date	Most Reasonable Impact Prediction	Issue Time of Prediction	Prediction Error	Minimized Error	$K \geq 6$ or 7 Alert Date Issued	Lead Time Between Alert and ICME Arrival
24 Oct. 2003 1529 UTC	24 Oct. 2003 1200 UTC, "mid-day on 24 Oct."	22 Oct. 2003 2240 UTC	3 hours 29 min	0 hours 0 min	24 Oct. 2003 1507 UTC	+22 min
28 Oct. 2003 0206 UTC	28 Oct. 2003 1200 UTC, "minor storm conditions on day two"	26 Oct. 2003 2200 UTC	9 hours 54 min	0 hours 0 min	none issued or required; no major or severe storm was observed	not applicable since an alert was not issued
29 Oct. 2003 0613 UTC	29 Oct. 2003 1200 UTC, "likely impact the earth's magnetic field by mid-day on day one"	28 Oct. 2003 2200 UTC	5 hours 47 min	0 hours 0 min	29 Oct. 2003 0623 UTC	-10 min
30 Oct. 2003 1640 UTC	31 Oct. 2003 0300 UTC, "impact from today's X10 flare will be assessed next period; predictions for days two and three will likely change considerably"	29 Oct. 2003 2200 UTC	10 hours 20 min	7 hours 20 min	30 Oct. 2003 1657 UTC	-17 min
4 Nov. 2003 0627 UTC	3 Nov. 2003 1200 UTC, "beginning on day one near the middle of the day"	2 Nov. 2003 2200 UTC	18 hours 27 min	12 hours 27 min	4 Nov. 2003 0634 UTC	-7 min

<sup>a</sup>Average time-of-arrival prediction error was 9 hours 35 min. Impact date was obtained from ground-level magnetometer data. Impact predictions were obtained from the daily "Report of Solar and Geophysical Activity" ([www.sec.noaa.gov/forecast.html](http://www.sec.noaa.gov/forecast.html)).  $K \geq 6$  or 7 alerts were obtained in real time from SEC via e-mail and documented in its Preliminary report and forecast of Solar Geophysical Data ([www.sec.noaa.gov/weekly](http://www.sec.noaa.gov/weekly)).

Table 4. Predictions of IPS Radio and Space Services Australia<sup>a</sup>

Observed ICME Impact Date	Most Reasonable Impact Prediction	Prediction Issue Time	Prediction Error	Minimized Error	Storm Alert Date/Time	Lead Time Between Alert and ICME Arrival
24 Oct. 2003 1529 UTC	24 Oct. 2003 0600 UTC, "early on 24th"	22 Oct. 2003 2330 UTC	9 hours 29 min	0 hours 0 min	24 Oct. 2003 1458 UTC	+31 min
28 Oct. 2003 0206 UTC	28 Oct. 2003 1800 UTC, "2nd half of UT day on 28 Oct."	26 Oct. 2003 2330 UTC	15 hours 54 min	9 hours 54 min	no alert issued or required; no major or severe storm was observed	not applicable since an alert was not issued
29 Oct. 2003 0613 UTC	29 Oct. 2003 1800 UTC, "2nd half of UT day on 29 Oct."	28 Oct. 2003 2211 UTC	11 hours 47 min	5 hours 47 min	29 Oct. 2003 0628 UTC	-15 min
30 Oct. 2003 1640 UTC	01 Nov. 2003 0000 UTC, "late on 31 Oct. or early on 01 Nov."	29 Oct. 2003 2330 UTC	31 hours 20 min	19 hours 20 min	first mention of storm on 30 Oct. at 2025 UTC by automated $K = 7$ detection	excluded
4 Nov. 2003 0627 UTC	4 Nov. 2003 1200 UTC, "around mid-day on 04 Nov."	2 Nov. 2003 2330 UTC	5 hours 33 min	0 hours 0 min	4 Nov. 2003 0607 UTC	+20 min

<sup>a</sup>Average time-of-arrival prediction error was 14 hours 49 min. Impact date was obtained from ground-level magnetometer data. Impact predictions and issued storm alerts are available in real time via e-mail and are archived at [www.ips.gov.au](http://www.ips.gov.au).

**Table 5.** Predictions of Geophysical Institute, University of Alaska at Fairbanks<sup>a</sup>

Observed Impact	HAFv.2		STOA		STOA-2		ISPM		Selected Prediction Error
	Impact Prediction	Prediction Error	Impact Prediction	Prediction Error	Impact Prediction	Prediction Error	Impact Prediction	Prediction Error	
24 Oct. 1529 UTC	25 Oct. 0300 UTC	11 hours 31 min	24 Oct. 1331 UTC	1 hour 58 min	24 Oct. 0840 UTC	6 hours 49 min	25 Oct. 0526 UTC	13 hours 57 min	8 hours 34 min
28 Oct. 0206 UTC	28 Oct. 0400 UTC	1 hours 54 min	28 Oct. 1812 UTC	16 hours 6 min	28 Oct. 2017 UTC	18 hours 11 min	29 Oct. 0541 UTC	27 hours 35 min	15 hours 57 min
29 Oct. 0613 UTC	30 Oct. 0200 UTC	19 hours 47 min	29 Oct. 1713 UTC	11 hours 0 min	29 Oct. 1833 UTC	12 hours 20 min	29 Oct. 1936 UTC	13 hours 23 min	14 hours 8 min
30 Oct. 1640 UTC	30 Oct. 2000 UTC	3 hours 20 min	31 Oct. 0319 UTC	10 hours 39 min	31 Oct. 1141 UTC	19 hours 01 min	30 Oct. 1933 UTC	2 hours 53 min	8 hours 58 min
4 Nov. 0627 UTC	04 Nov 0300 UTC	3 hours 27 min	4 Nov. 0412 UTC	2 hours 15 min	4 Nov. 2138 UTC	15 hours 11 min	4 Nov. 0413 UTC	2 hours 14 min	5 hours 47 min

<sup>a</sup>Average time-of-arrival prediction errors were 8 hours 0 min (HAFv.2), 8 hours 24 min (STOA), 14 hours 18 min (STOA-2), and 12 hours 0 min (ISPM). Overall average prediction error was 10 hours 41 min.

arrival prediction based on the suite of predictions issued for each event. This was done by selecting the average of the four published time-of-arrival predictions for STOA, STOA-2, ISPM, and HAFv.2, (shown in the “selected” column of Table 5). Earlier studies of these models have shown that time-of-arrival errors of between 9.8 and 11.6 hours are to be expected [Cho *et al.*, 2003]. Our most reasonable average error of 10.68 hours for the suite of models is therefore in good agreement with these findings.

[30] The most uncertain prediction for which a preferred time of arrival was difficult to determine was issued by the Space Environment Center on 29 October. Its daily summary report (a copy is available from sec@sec.noaa.gov) stated that

The potential geomagnetic impact from today’s X10 flare will be assessed next period; predictions for days two and three will likely change considerably.

[31] Unfortunately, the ICME from this event arrived before SEC’s “next period.” We are therefore left with only the last snippet of this statement for clues as to when the forecaster thought the disturbance might arrive. These snippets suggest that the SEC forecaster believed that the ICME would impact on days 2 and 3 (31 October and 1 November). We have therefore assigned an impact time of 0300 UTC on 31 October as an estimate, reasoning that the forecaster would have preferred an early UTC day impact on 31 October.

### 3.1. Time-of-Arrival Prediction Results

[32] Figure 7 provides a side-by-side comparison of the most reasonable time-of-arrival predictions for each of the forecast centers and for the five strongest space weather events of 24 October through 4 November. Clearly, the predictions from STD were associated with the lowest prediction errors.

**Table 6.** Solar Influences Data Center (SIDC) Belgium Predictions<sup>a</sup>

Observed ICME Impact Date	Most Reasonable Impact Prediction	Prediction Issue Time	Prediction Error	Minimized Error
24 Oct. 2003 1529 UTC	24 Oct. 2003 1200 UTC, “to become geoeffective by 24 Oct.”	23 Oct. 2003 1333 UTC	3 hours 29 min	0 hours 0 min
28 Oct. 2003 0206 UTC	28 Oct. 2003 0600 UTC, “early on 28 Oct.”	27 Oct. 2003 1230 UTC	3 hours 54 min	0 hours 0 min
29 Oct. 2003 0613 UTC	30 Oct. 2003 1200 UTC, “major to severe magnetic storm on Thursday 30 Oct.”	28 Oct. 2003 1230 UTC	29 hours 47 min	17 hours 47 min
30 Oct. 2003 1640 UTC	31 Oct. 2003 0000 UTC, “tonight or early tomorrow (31Oct.)”	30 Oct. 2003 1351 UTC	7 hours 20 min	1 hour 20 min
4 Nov. 2003 0627 UTC	4 Nov. 2003 1200 UTC, “may arrive on 04 November”	3 Nov. 2003, 1227 UTC	5 hours 33 min	0 hours 0 min

<sup>a</sup>Average time-of-arrival prediction error was 10 hours 1 min. Impact date was obtained from ground-level magnetometer data. Impact predictions are available via e-mail and at www.sidc.oma.be.

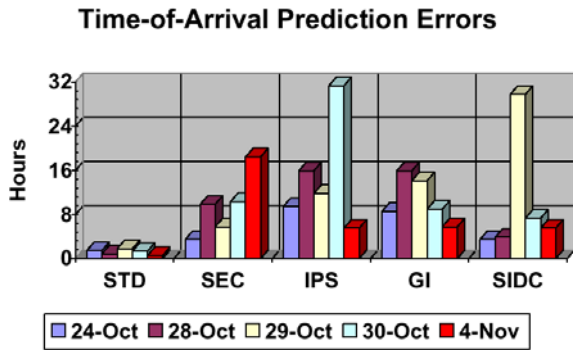


Figure 7. Nominal (most reasonable) time-of-arrival prediction errors for each of the five events studied.

[33] The most difficult events to predict are determined by summing together the time-of-arrival errors for each of the events and for all of the forecast centers, as shown in Figure 8. As Figure 8 illustrates, the most difficult ICME impacts to predict were the fastest transit events of 29 and 30 October. This is probably no coincidence. The ICME that impacted on 29 October made it to the Earth in only 18.82 hours, while the event of 30 October required only 19.5 hours (SEC, 2003). There is very little climatological information for events with such high velocities. The lack of useful historic information may have hindered the formation of accurate predictions. In addition, the lower-energy signature of the X10/2B flare of 29 October may have contributed to the poor prediction performance of the 30 October ICME impact. That solar flare covered roughly half the area, had a slower estimated type II shock velocity, and was 1.7 times less intense in X rays than the preceding class X17+/4B event of 28 October. These weaker characteristics may have led forecasters to expect a lower ICME velocity. Although this seems reasonable, the deceleration curve of the ICME was probably flatter than expected given the path the ICME would have taken through the higher-velocity wake of the fast X17+/4B solar flare-associated ICME.

[34] Figure 9 shows the accumulated most reasonable prediction errors of each forecast center and reveals which forecast centers performed the best by scoring the lowest

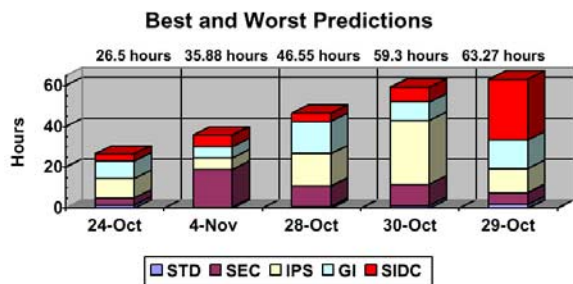


Figure 8. Best and worst predicted events and the error contributions of each prediction center. Thin slabs represent good prediction performance.

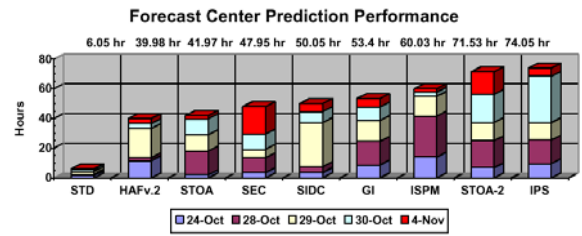


Figure 9. Cumulative most reasonable prediction errors for each space weather forecast center, indicating the best performing forecast centers for the five strongest ICME impact events of October and November 2003. Lower error values (thinner slabs) indicate higher prediction accuracy.

accumulated errors. It illustrates that several of GI's numerical models outperformed many of the forecast center predictions. In particular, the STOA and HAFv.2 models were consistently more accurate. This interesting result suggests that, with the exception of STD, the other forecast centers may have been able to improve their performance by relying solely on the guidance of the HAFv.2 model.

[35] Figure 10 is an accumulation of the minimized time-of-arrival errors for each of the forecast centers. The minimized prediction errors are far more objective (even overly optimistic) and represent the smallest possible errors that could be assigned to each prediction on the basis of the limitations of the prediction statements. For example, if a prediction calls for an impact "on day 2" (lacking any additional time-of-arrival information) and the ICME impacts the Earth any time on day 2, a minimized prediction error of 0 (a perfect prediction) is assigned for that event. On the other hand, if the prediction is slightly more informative and calls for an impact "during the latter-half of day 2" and the ICME impacts the Earth during the first half of the day, then a minimized prediction error representing the difference between the observed impact time and 1200 UTC is assigned for that



Figure 10. Estimated best possible prediction performance of each space weather forecast center (in ascending order) determined by accumulating the lowest possible prediction errors for each forecast center and for each of GI's shock arrival model predictions. The minimized error for GI is defined as the accumulated time-of-arrival errors for the closest of the four model predictions to the observed ICME impact times.

event. For GI the minimized error is determined by using the time-of-arrival prediction result from the most accurate model for each of the events. The “minimized error” columns of Tables 2–6 represent the minimized prediction errors in Figure 10.

[36] It is interesting to note that GI’s accumulated minimized prediction errors were at least as accurate as the minimized predictions issued by each of the other forecast centers (excluding STD). This means that, with the exception of STD, the predictions from the other forecast centers for the five strongest ICME impacts were essentially no better than the predictions from the best performing models operated by GI.

[37] It is also interesting to note that STD’s time-of-arrival prediction errors were more than 3 times smaller than the minimized errors of the other forecast centers. Possible reasons for this are discussed in section 3.2.

### 3.2. Sources of Prediction Inaccuracies

[38] The success of any solar wind shock time-of-arrival prediction model is inherently dependent on the quality of the data input into the model. Unfortunately, many of the required model inputs cannot be easily or accurately answered. For example, a fundamental quantity required by every model is a description of the initial velocity of the coronal mass ejection. The type II shock velocity inferred from ground-based observations of sweep frequency radio bursts [Gopalswamy, 2000] is typically used as an estimate for this parameter. However, this measurement is strongly dependent on coronal density models which are known to have deficiencies [Sun *et al.*, 2002]. In addition, there are fundamental debates concerning the true origin of the type II emissions [Shanmugaraju *et al.*, 2003] and whether they are always related to ICMEs. If the type II input parameter is inaccurate, the prediction output by the model will invariably suffer.

[39] Numerous additional error sources also exist, such as the shape and precise trajectory of the coronal mass ejection [Gopalswamy and Kaiser, 2002], the duration of the driven phase of the shock, and how the structure of the solar wind upstream of the shock may affect its character. At the present time the tools simply do not exist to determine many of these required physical characteristics with absolute certainty. Thus many assumptions and forecaster-dependent “best guesses” are involved in modeling ICME impacts.

[40] Studies of model performance [Cho *et al.*, 2003; Smith *et al.*, 2000] have shown that the accumulated modeling errors generally result in time-of-arrival predictions that are accurate to within about 10–12 hours. Each forecast center attempts to minimize the errors by choosing input parameters that seem reasonable to each forecaster.

[41] As this study has demonstrated, it is possible to significantly exceed the accuracy of standard interplanetary shock time-of-arrival prediction models if the forecaster is careful in selecting model input parameters. The success of Solar Terrestrial Dispatch in maintaining significantly lower errors during the five strongest ICME impacts is attributed to a judicious selection of model

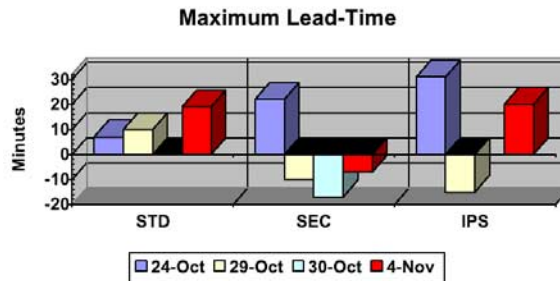


Figure 11. Maximum lead time, defined as the time measured from the arrival of an ICME at the ACE spacecraft to the issuance of a geomagnetic storm alert by Solar Terrestrial Dispatch, the Space Environment Center, and Ionospheric Prediction Service Radio and Space Services Australia. Higher positive values are the most desirable.

inputs from the available data rather than an unusually accurate modeling method.

### 4. Maximum Alert Lead Time Performance

[42] This section discusses the alert lead time performance of STD and SEC to the NPCC control centers. The alert lead time associated with IPS is also examined. The “maximum alert lead time” is defined as the maximum amount of response time the NPCC control centers have from the moment a geomagnetic storm alert is issued to the moment the ICME impacts the Earth and produces measurable enhancements in geomagnetic activity. This definition helps to identify how rapidly each forecast center responds to the arrival and identification of storm-capable ICMEs.

[43] Four of the five ICME events considered in this study produced relatively prompt major to severe geomagnetic storm conditions (planetary geomagnetic  $K$  indices of 6 or greater) following their arrivals. These include the ICME impacts of 24 October, 29 October, 30 October, and 4 November. The event of 28 October was not strong enough to generate prompt geomagnetic storm alerts from STD, SEC, or IPS.

[44] The strong forward shock of the 29 October ICME drove moderately strong GICs of between 10 and 20 A in the NPCC region when it impacted the Earth’s magnetosphere. The relevant importance of the rapid notification of shock arrivals is thereby demonstrated.

[45] Tables 2 and 3 provide comparative information concerning the issuance of major to severe geomagnetic storm alerts to the NPCC region by STD and SEC. Table 4 contains comparative information from IPS. The alerts disseminated by SEC were distributed throughout the North America Energy Reliability Council, which encompasses all power companies in North America, while those of STD were disseminated only to the NPCC.

[46] The maximum lead time for each of the four qualifying events is illustrated graphically in Figure 11. The maximum lead time for the 29 October ICME is of partic-

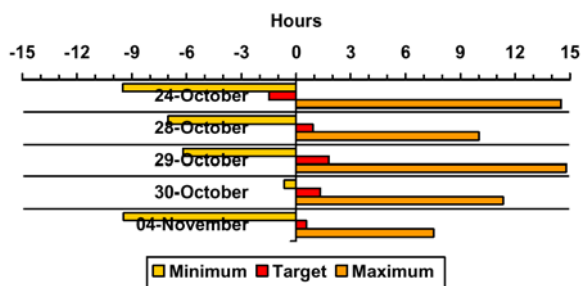


**Figure 12.** Impact prediction windows from STD for all five of the studied events. The central 0-hour line represents the time the ICME impacted the Earth and produced a sudden magnetic impulse. Bars represent the difference (in hours) between the observed impact time and the predicted (preferred) “target” impact time, the predicted earliest “minimum” time the disturbance might impact, and the predicted latest “maximum” time the disturbance might arrive.

ular interest because of the size of the associated leading solar wind shock front and its ability to produce notable GIC activity within the NPCC region. Solar Terrestrial Dispatch issued a severe storm alert 10 min before this shock front impacted the Earth. The shock traveled from ACE to the Earth in only 14 min, which is less than half of the time that is normally required for an average “high”-velocity ICME to reach the Earth from the L1 point. IPS and SEC issued their alerts 15 and 10 min, respectively, after the disturbance had impacted the Earth and at least 8 min after moderately strong GIC activity had first been detected on the power grids.

[47] Note in Figure 11 that the Solar Terrestrial Dispatch lead time for the 30 October event is plotted at the 0 min mark to signify the fact that STD was still in a severe geomagnetic storm alert mode when the 30 October ICME impacted the Earth. STD was therefore not required to send out an alert (although a notice of the shock arrival was communicated to the control centers). The Space Environment Center canceled its severe storm alert less than 1 hour before this disturbance impacted the Earth. SEC then had to reinstate the severe storm alert after the ICME arrived, which it did 17 min after the disturbance impacted the Earth. IPS does not mention the arrival of the ICME in its products until 2025 UTC on 30 October, after its systems detected a period of severe geomagnetic storming. The IPS lead time for this event is therefore excluded from the plot in Figure 11.

## 5. Use of Impact Prediction “Windows”

[48] For each ICME impact prediction it is useful to specify the extremes of the possible maximum and minimum arrival times (an impact window). STD is the only forecast center in this study that produced impact prediction windows for each of the ICME events. Its prediction windows for the events of 24 October to 4 November are shown in Figure 12.

[49] It is interesting to note how the impact prediction window for the fast transit event of 30 October differed from the other prediction windows. In particular, STD’s predicted earliest (“minimum”) time of arrival for this event was very close to the predicted “target” time of arrival. This was the result of the forecaster correctly reasoning that the observed lower plane-of-sky velocity (and the overall lower energy profile of the solar flare event of 29 October) would not involve an ICME with a faster transit velocity than the earlier fast transit event of 29 October. Narrowing the prediction window in this manner provides obvious advantages to space weather consumers, where smaller (or larger) minimum or maximum bars relative to the predicted target time of arrival implicitly indicate greater (or lesser) confidence in the predicted ICME times of arrivals.

## 6. Conclusions

[50] The prediction performance of five global space weather forecast centers was studied in relation to the five strongest ICME disturbances of 24 October through 4 November 2003. Performance was measured in terms of the accuracy of the forecast centers in predicting the times of arrivals of the ICMEs. The lead time between the first issued geomagnetic storm alert and the first measured geomagnetic response to the impact of the ICME was also examined.

[51] Solar Terrestrial Dispatch had the best performance in all respects, with accumulated time-of-arrival prediction errors at least 3 times lower than the next best performer. The other space weather forecast centers performed about as well as the HAFv.2 and STOA models. Of the four numerical prediction models operated by GI, the HAFv.2 model provided the best guidance.

[52] The most problematic events to predict were the fast transit events of 29 and 30 October. This is reasonable given the scarcity of historic events of comparable magnitudes on which to base predictions.

[53] Some important recommendations most space weather forecast centers should consider implementing include the following.

[54] 1. Detailed ICME impact predictions should be released whenever sufficient data are available to formulate a forecast, rather than waiting to integrate the results into daily products that are issued at fixed times each day.

[55] 2. The direct use of published type II shock velocities in ICME propagation prediction models should be used cautiously as an initial ICME velocity estimate. The type II estimates for each of the events in this study under-predicted (sometimes significantly) the true velocity of the ICME forward shocks.

[56] 3. Impact prediction “windows” should be included in predictions. Impact windows will allow users of space weather services to better plan for disturbed conditions.

[57] **Acknowledgments.** The author gratefully acknowledges the Space Environment Center for providing the data and core services that made this study and all supplementary prediction services

possible. The vital role of the ACE operations teams and the SOHO/LASCO science teams in measuring, analyzing, and notifying the forecasting community of potential coronal mass ejection threats is also recognized and appreciated. The forecast and support staff at IPS and SIDC are also acknowledged for their work in providing timely data. The kind assistance of Ronald Van der Linden at SIDC, Richard Thompson at IPS, Christopher Balch at SEC, and Murray Dryer (who works with the research team associated with the GI) is also gratefully acknowledged. The author also thanks the reviewers for their thoughtful insight and assistance.

## References

- Araki, J. (1977), Global structure of geomagnetic sudden commencements, *Planet. Space Sci.*, 25, 373.
- Cho, K.-S., Y.-J. Moon, M. Dryer, C. D. Fry, Y.-D. Park, and K.-S. Kim (2003), A statistical comparison of interplanetary shock and CME propagation models, *J. Geophys. Res.*, 108(A12), 1445, doi:10.1029/2003JA010029.
- Czech, P., S. Chano, H. Huynh, and A. Dutil (1992), The Hydro-Quebec system blackout of 13 March 1989: System response to geomagnetic disturbance, in *Proceedings of Geomagnetically Induced Currents Conference, Millbrae, California, USA, November 8–10, 1989, Rep. TR-10450*, p. 19.1, Electr. Power Res. Inst., Palo Alto, Calif.
- Dryer, M., and D. F. Smart (1984), Dynamical models of coronal transients and interplanetary disturbances, *Adv. Space Res.*, 4, 291.
- Fry, C. D. (1985), The three-dimensional geometry of the heliosphere: Quiet time and disturbed periods, Ph.D. dissertation, Univ. of Alaska, Fairbanks.
- Fry, C. D., W. Sun, C. S. Deehr, M. Dryer, Z. Smith, S.-I. Akasofu, M. Tokumaru, and M. Kojima (2001), Improvements to the HAF solar wind model for space weather predictions, *J. Geophys. Res.*, 106, 20,985.
- Gonzalez, W. D., and B. T. Tsurutani (1987), Criteria of interplanetary parameters causing intense magnetic storms ( $Dst < 100$  nT), *Planet. Space Sci.*, 35, 1101.
- Gonzalez, W. D., J. A. Joselyn, Y. Kamide, H. W. Kroehl, G. Rostoker, B. T. Tsurutani, and V. M. Vasyliunas (1994), What is a geomagnetic storm?, *J. Geophys. Res.*, 99, 5771.
- Gonzalez, W. D., A. L. Chua de Gonzalez, A. Dal Lago, B. T. Tsurutani, J. K. Arballo, G. K. Lakhina, B. Buti, C. M. Ho, and S. T. Wu (1998), Magnetic cloud field intensities and solar wind velocities, *Geophys. Res. Lett.*, 25, 963.
- Gopalswamy, N. (2000), Type II solar radio bursts, in *Radio Astronomy at Long Wavelengths, Geophys. Monogr. Ser.*, vol. 119, edited by R. G. Stone et al., p. 123, AGU, Washington, D. C.
- Gopalswamy, N., and M. L. Kaiser (2002), Solar eruptions and long wavelength radio bursts: The 1997 May 12 event, *Adv. Space Res.*, 29, 307.
- Gosling, J. T., and D. J. McComas (1987), Field line draping about fast coronal mass ejecta: A source of strong out-of-the-ecliptic interplanetary magnetic fields, *Geophys. Res. Lett.*, 14, 355.
- Gosling, J. T., D. J. McComas, J. L. Phillips, and S. J. Bame (1991), Geomagnetic activity associated with Earth passage of interplanetary shock disturbances and coronal mass ejections, *J. Geophys. Res.*, 96, 7831.
- Hakamada, K., and S.-I. Akasofu (1982), Simulation of three-dimensional solar wind disturbances and resulting geomagnetic storms, *Space Sci. Rev.*, 31, 3.
- Lambour, R. L., A. J. Coster, R. Clouser, L. E. Thornton, J. Sharma, and T. A. Cott (2003), Operational impacts of space weather, *Geophys. Res. Lett.*, 30(3), 1136, doi:10.1029/2002GL015168.
- Lewis, D., and M. Dryer (1987), Shock-time-of-arrival model (STOA-87), NOAA/SEL contract report (systems documentation), U. S. Air Force Air Weather Serv., Scott AFB, Ill.
- Lindsay, G. M., J. G. Luhmann, C. T. Russell, and J. T. Gosling (1999), Relationship between coronal mass ejection speeds from coronagraph images and interplanetary characteristics of associated interplanetary coronal mass ejections, *J. Geophys. Res.*, 104, 12,515.
- Moon, Y.-J., M. Dryer, Z. Smith, U.-D. Park, and K.-S. Cho (2002), A revised shock time of arrival (STOA) model for interplanetary shock propagation: STOA-2, *Geophys. Res. Lett.*, 29(10), 1390, doi:10.1029/2002GL014865.
- Ogilvie, K. W., L. F. Burlaga, and T. D. Wilkerson (1968), Plasma observations on Explorer 34, *J. Geophys. Res.*, 73, 6809.
- Richardson, I. G., E. W. Cliver, and H. V. Cane (2001), Sources of geomagnetic storms for solar minimum and solar maximum conditions during 1972–2000, *Geophys. Res. Lett.*, 28, 2569.
- Russell, C. T., M. Grinskey, and S. M. Petriner (1994), Sudden impulses at low latitude stations: Steady state response for southward interplanetary magnetic field, *J. Geophys. Res.*, 99, 13,403.
- Shanmugaraju, A., Y.-J. Moon, M. Dryer, and S. Umaphathy (2003), An investigation of solar maximum metric type II radio bursts: Do two kinds of coronal shock sources exist?, *Sol. Phys.*, 215, 161.
- Siscoe, G. L., V. Formisano, and A. J. Lazarus (1968), A calibration of the magnetopause, *J. Geophys. Res.*, 73, 4869.
- Smart, D. F., and M. A. Shea (1985), A simplified model for timing the arrival of solar-flare-initiated shocks, *J. Geophys. Res.*, 90, 183.
- Smart, D. F., M. A. Shea, W. R. Barron, and M. Dryer (1984), A simplified technique for estimating the arrival time of solar flare-initiated shocks, in *Proceedings of STIP Workshop on Solar/Interplanetary Intervals*, edited by M. A. Shea, D. F. Smart, and S. McKenna-Lawlor, p. 139, Book Crafters, Chelsea, Mich.
- Smart, D. F., M. A. Shea, M. Dryer, A. Quintana, L. C. Gentile, and A. A. Bathurst (1986), Estimating the arrival time of solar flare-initiated shocks by considering them to be blast waves riding over the solar wind, in *Proceedings of the Symposium on Solar-Terrestrial Predictions*, edited by P. Simon, G. R. Heckman, and M. A. Shea, p. 471, U.S. Govt. Print. Off., Washington, D. C.
- Smith, Z. K., and M. Dryer (1995), The interplanetary shock propagation model: A model for predicting solar-flare-caused geomagnetic sudden impulses based on the 2-1/2D MHD numerical simulation results from the Interplanetary Global Model (2D IGM), *NOAA Tech. Memo. ERL/SEL-89*, Natl. Ocean. Atmos. Admin., Silver Spring, Md.
- Smith, Z., M. Dryer, E. Ort, and W. Murtagh (2000), Performance of interplanetary shock prediction models: STOA and ISPM, *J. Atmos. Sol. Terr. Phys.*, 62, 1265.
- Sun, W., M. Dryer, C. D. Fry, C. S. Deehr, Z. Smith, S.-I. Akasofu, M. D. Kartalev, and K. G. Grigorov (2002), Real-time forecasting of ICME shock arrivals at L1 during the “April Fool’s Day” Epoch: 28 March–21 April 2001, *Ann. Geophys.*, 20, 937.
- Thomson, N. R., C. J. Rodger, and R. L. Dowden (2004), Ionosphere gives size of greatest solar flare, *Geophys. Res. Lett.*, 31, L06803, doi:10.1029/2003GL019345.
- Tsurutani, B. T., W. D. Gonzalez, F. Tang, S. I. Akasofu, and E. J. Smith (1988), Solar wind southward  $B_z$  features responsible for magnetic storms of 1978–1979, *J. Geophys. Res.*, 93, 8519.
- Vlasov, V. I. (1988), Radio-astronomical measurement of the velocity of interplanetary shock waves, *Geomagn. Aeron.*, Engl. Transl., 28, 1.
- Vlasov, V. I. (1992), Traveling interplanetary disturbances from radio astronomical data, in *Proceedings of the First SOLTIP Symposium*, vol. 1, edited by S. Fischer and M. Vandas, p. 273, Astron. Inst. of the Czech. Acad. Sci., Prague.
- Yurchyshyn, V., H. Wang, and V. Abramenko (2004), Correlation between speeds of coronal mass ejections and the intensity of geomagnetic storms, *Space Weather*, 2, S02001, doi:10.1029/2003SW000020.

C. Oler, Solar Terrestrial Dispatch, P.O. Box 357, Stirling, Alberta, Canada T0K 2E0. (oler@spacew.com)